

## Micro-focus X-ray scanning on layers of smectic superstructures

I. Gurke<sup>1</sup>, \*C. Wutz<sup>1</sup>, D. Gieseler<sup>1</sup>, B. Janssens<sup>1</sup>,  
F. Heidelberg<sup>2</sup>, C. Riekell<sup>2</sup>, H.R. Kricheldorf<sup>1</sup>

<sup>1</sup> Universität Hamburg, Institut für Technische und  
Makromolekulare Chemie, Hamburg, Germany

<sup>2</sup> European Synchrotron Radiation Facilities, BL 1, ID 13,  
Grenoble, France

**Abstract:** The investigated main chain poly(ester imide)s (PEI) form smectic layers with different superstructures due to a nanophase separation of the rigid mesogens and flexible spacers, which give rise to X-ray reflections in the small angle region ( $2\theta = 1-6^\circ$ ;  $d=2-8$  nm). The novel micro-focus X-ray scanning technique at the beamline ID13 (ESRF, France) enables a visualisation of the local orientation of smectic layers in different morphologies such as bâtonnets and spherulites. Previous investigations of the spherulites formed from PEI by optical and electron microscopy, and SAXS indicated a negative birefringence and a lamellar internal structure. The particular feature of these spherulites is their internal smectic layer structure. The present X-ray scanning experiments reveal a radial arrangement of the smectic layers within the spherulite. Furthermore, the micro-beam scanning experiments provide maps of the molecular orientation in different smectic LC-textures. The internal  $S_C$ -order of a single bâtonnet ( $10 * 90 \mu\text{m}$ ) could be examined.

### 1. Introduction

Main chain polymers consisting of a regular sequence of rigid, polar mesogens and non-polar, flexible spacers tend to form smectic layer structures in different mesophases. The degree of order achieved among the mesogens depends on the chemical structure and the thermal treatment of the polymer. While nematic phases exhibit only one-dimensional orientational order, the mesogens achieve a layer order in smectic phases. In addition to the smectic LC-phases  $S_A$  and  $S_C$  a number of so-called higher-ordered or smectic-crystalline phases exist, which are classified as  $S_B$ ,  $S_E$ ,  $S_F$ ,  $S_H$  etc. depending on the lateral order of the mesogens and their orientation with respect to the layer plane<sup>1</sup>. In these phases, the mesogens exhibit long range positional order within the layers but not among them<sup>2</sup>.

Upon cooling, thermotropic polymers form LC-phases with typical Schlieren- or bâtonnet textures, which can transform into smectic-crystalline phases during further cooling. With increasing spacer length, the temperature interval of the LC-phase becomes narrower. If the LC-phase is lost completely, the smectic-crystalline phase develops directly from the isotropic matrix forming spherulites<sup>3</sup>. In contrast to conventional spherulites of semi-crystalline polymers,

they exhibit an internal smectic-crystalline layer structure, giving rise to a SAXS reflection at  $2\theta = 1-6^\circ$  in addition to the long period reflection of 15-30 nm in the "real SAXS". In the present work we investigated the local arrangement of the smectic layers within different mesophase morphologies by means of a X-ray micro-focus camera.

### 2. Experimental Part

#### 2.1 Measurements

Whereas the synchrotron X-ray beamlines X27C (NSLS, USA) and A2 (HASYLAB, Germany) allow investigations of structural changes during processing of polymers in real time, the micro-focus scanning technique at the beamline ID13 (ESRF, France)<sup>4</sup> provides a tool for visualising the spatial change of molecular order in the polymer morphology. We used this novel technique to probe different smectic mesophase structures ( $d = 2-8$  nm) by the azimuthal distribution of the X-ray reflection in the small angle range ( $2\theta = 1-6$ ). Automatic changing of the beam position in  $2\mu\text{m}$  steps and data acquisition by 2D-Imaging provides spatially resolved X-ray frame mapping of the samples in a relatively short time.

#### 2.1 Investigated Matter

The poly(ester imide)s (PEI) of the chemical structure **1** and **2** (Figure 1) represent excellent model compounds for the investigation of smectic layer structures. Previous DSC and X-ray measurements<sup>5</sup> revealed that PEI-1 displays metastable, monotropic LC-phases ( $S_A$ ,  $S_C$ ) with a bâtonnet, fan-shaped or Schlieren-texture. Upon further cooling, the transition into higher-ordered, smectic-crystalline phases ( $S_E$ ,  $S_H$ ) occurs. PEI-2 forms smectic-crystalline spherulites directly from the isotropic melt without any intermediate LC-phase.

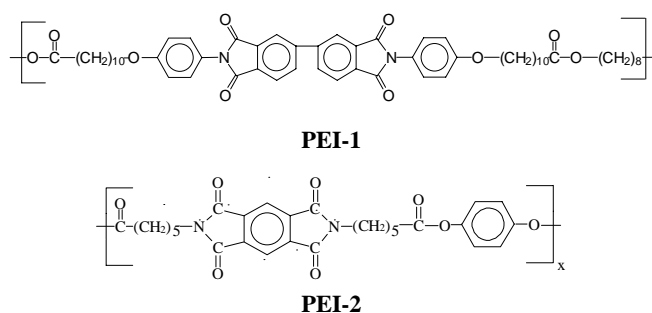


**Figure 1.** Chemical structures of the PEI-1 and PEI-2.

## 2.2 Experimental technique

At the micro-focus beamline ID13 at ESRF the synchrotron-X-ray beam is focussed by means of a total reflection glass capillary. The beam size is down to  $2\ \mu\text{m}$  FWHM at sample position. The beam exhibits a divergence of 3 mrad. The wavelength of the X-ray beam is  $0.9\ \text{\AA}$  with an integer flux of  $10^{10}$  photons per second (flux density:  $10^9\ \text{photons s}^{-1}\ \mu\text{m}^{-2}\ \text{mA}^{-1}$ ). The distance between sample and capillary was 1 mm. In order to reduce background scattering, an aperture slit of  $10\ \mu\text{m}$  diameter was set up between capillary and sample<sup>6</sup>. Data acquisition was realised with an 110 mm CCD-camera (Photonic Science; MarCCD). The distance between detector and sample varied between 100 and 550 mm.

## 2.3 Sample preparation

The polymers were heated to the isotropic phase between Kapton® foils, pressed into thin ( $<10\ \mu\text{m}$ ) films, cooled to the respective mesophase formation temperature, kept there isothermally, and quenched rapidly into ice-water. In PEI-1, bâtonnets of large dimensions (Figure 2) and Schlieren-textures (Figure 3) were obtained by annealing the sample in the temperature range of the respective LC-phase. Smectic spherulites (Figure 4 and 5) were grown by isothermal crystallisation of a PEI-2 film. The samples were fixed on a goniometer head and positioned normal to the incident beam. Sample positioning was realised by microscope guarding.

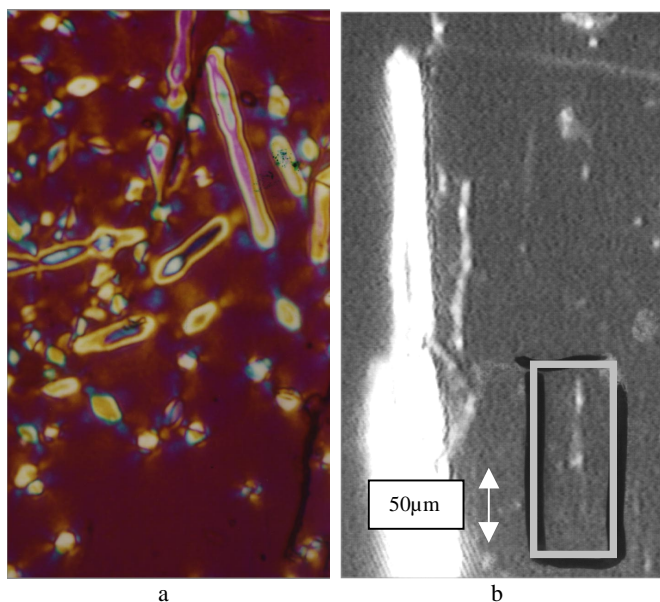


**Figure 2.** Polar micrograph of PEI-1 bâtonnets after 30 min at  $T = 245^\circ\text{C}$ ; (a) and online thermo-print (b); scanned area is marked.

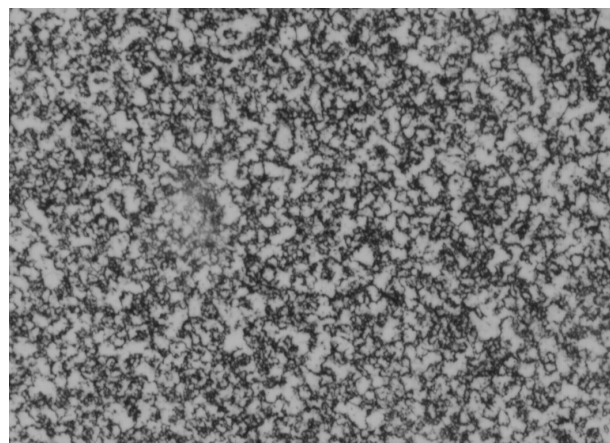


**Figure 3.** Schlieren-texture of PEI-1; micrograph between crossed polars

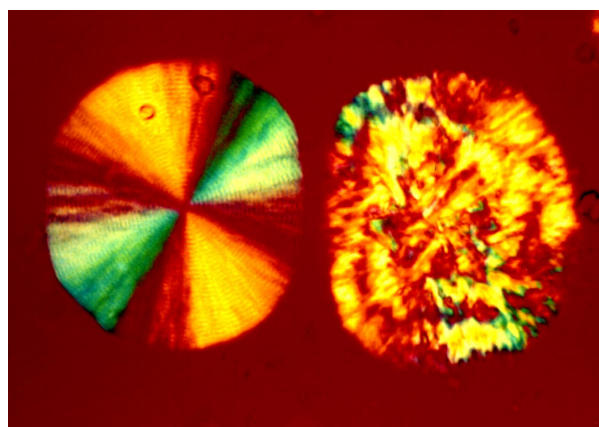


**Figure 4.** Spherulites of PEI-2 grown from the isotropic melt at  $T_c = 243^\circ\text{C}$ ; micrograph between crossed polars

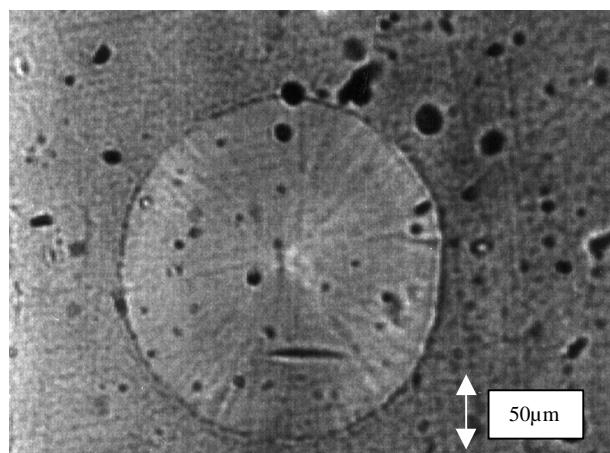


**Figure 5.** Spherulite of PEI-2 grown from the isotropic melt at  $T_c = 243^\circ\text{C}$ ; thermo-print at the experiment.

### 3. Results

#### 3.1 Smectic Schlieren-texture of PEI-1

The PEI-1 exhibits an enantiotropic smectic LC-Phase in a temperature range between  $T = 242$  and  $261^\circ\text{C}$ . In order to analyse the spatial change of the director, the smectic LC-phase was melt-pressed, quenched into the glassy state and the resulting Schlieren-texture was scanned by the micro-focus X-ray beam. As an example, Figure 6a-c shows three 2D-SAXS-patterns with oriented layer reflections of  $d=6$  nm spacing at different sample positions. The corresponding arrangement of the smectic layers is sketched above. In Figure 6a the beam covers virtually a single domain resulting in one pair of layer reflections. The domain boundary in Figure 6b gives rise to multiple reflections, whereas the poor orientation in Figure 6c indicates a spread of the director field.

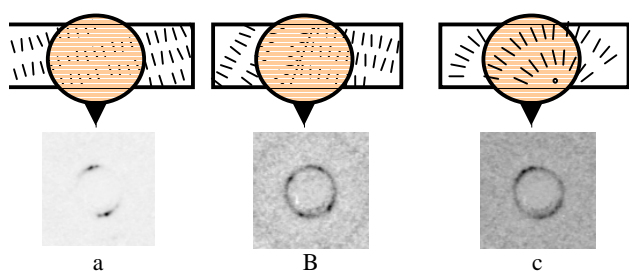


**Figure 6.** SAXS-patterns at different positions of a PEI-1 LC-texture (bottom) and corresponding arrangement of smectic layers (top). The beam covers one domain (a); two domains (b) and a spread (c).

The evaluation of SAXS patterns (not depicted) registered from an  $20 * 20 \mu\text{m}$  array of a PEI-1 Schlieren-texture (Figure 3) gives a fingerprint of the director field (Figure 7). In this way, splay, bends, and inversion walls at domain boundaries can be visualised.

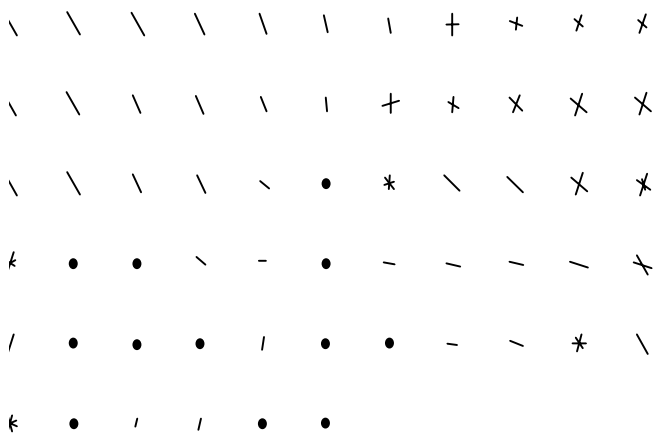


**Figure 7.** „Fingerprint“ of a director field ( $20 * 20 \mu\text{m}$ ) in PEI-1, step size  $2\mu\text{m}$ ; lines indicate preferred orientation of smectic layers.

Mapping of the PEI-1 Schlieren-texture by an array of SAXS-diagrams provides information on the domain structure by the following parameters:

- Domain size
- Type of defects
- Density of defects (disclinations)
- Gradient of defects (distorsions)

Figure 8 depicts the azimuthal distribution of the SAXS-reflection intensity from a horizontal scan (x-direction) through a PEI-1 sample at two different vertical (y) positions.

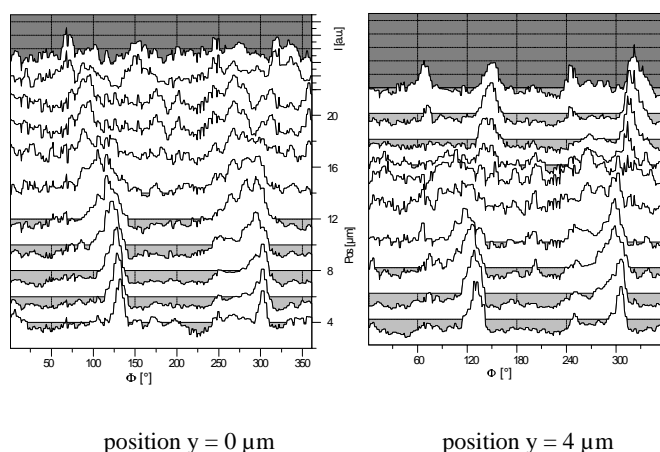


**Figure 8.** Micro-focus scanning of LC-glass from PEI-1; array of  $20 * 10 \mu\text{m}$ , steps of  $2\mu\text{m}$ ; azimuthal intensity versus sample position (x-axes) at two y-positions.

The evaluated parameters of the local domain structure are:

- Gradient of distortion:  $\phi = 3^\circ / \mu\text{m}$ .
- Thickness of domain interface:  $4-5\mu\text{m}$ .
- Average density of disclinations:  $2.5 * 10^{-3} \mu\text{m}^{-2}$

#### 3.2 Smectic Bâtonnets

During slow cooling of PEI-1, bâtonnets of about  $100 \mu\text{m}$  developed. Rapid quenching of the sample produces a fine grainy LC-texture in the surrounding matrix and freezes this morphology. Within the bâtonnet (Figure 9a) the micro-focus X-ray diagram displays a 4-point pattern of the layer reflection at  $2\Theta = 1.4^\circ$  ( $d = 6$  nm) in the SAXS and an equatorial amorphous halo in the WAXS, indicating local orientation. In contrast, the fine grainy matrix with a domain size below  $1 \mu\text{m}$  appears isotropic in the X-ray patterns in Figure 9b.

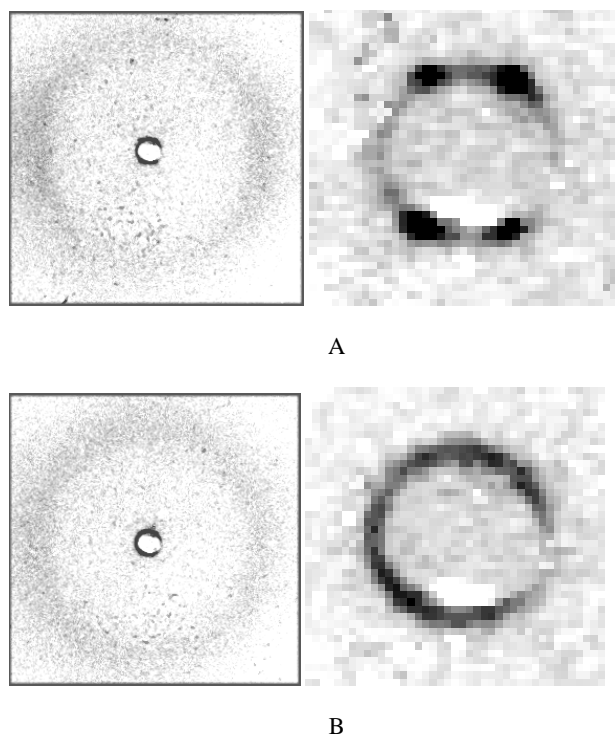


**Figure 9.** WAXS (left) and SAXS (right) of a PEI-1 LC-texture. Oriented scattering patterns within the bâtonnet (a), isotropic scattering from the fine grainy matrix (b).

Figure 10 represents a map of 7\*15 SAXS-diagrams scanning the bâtonnet sample in 2  $\mu\text{m}$  steps. The azimuthal distribution of the SAXS and WAXS (not depicted) at different sample positions provides the following information on the investigated structure.

This bâtonnet of PEI-2 is a symmetrical shape of a frozen smectic LC-phase ( $S_C$ ). The equatorial WAXS-halo indicates a preferred orientation of the molecules parallel to the axis of the bâtonnet. Due to the average staggering of adjacent mesogens in the  $S_C$ -phase, the smectic layer adopt an inclined orientation with respect to the bâtonnet axis, resulting in a 4-point SAXS pattern. At the interface between bâtonnet and matrix, the intensity distribution becomes asymmetrical. At the tip of the bâtonnet, a meridional layer reflection is observed in the SAXS, indicating that the smectic layer normals are oriented parallel to the bâtonnet axis ( $S_A$ -order). Due to the smectic poly-domain structure, the matrix appears isotropic in the SAXS.

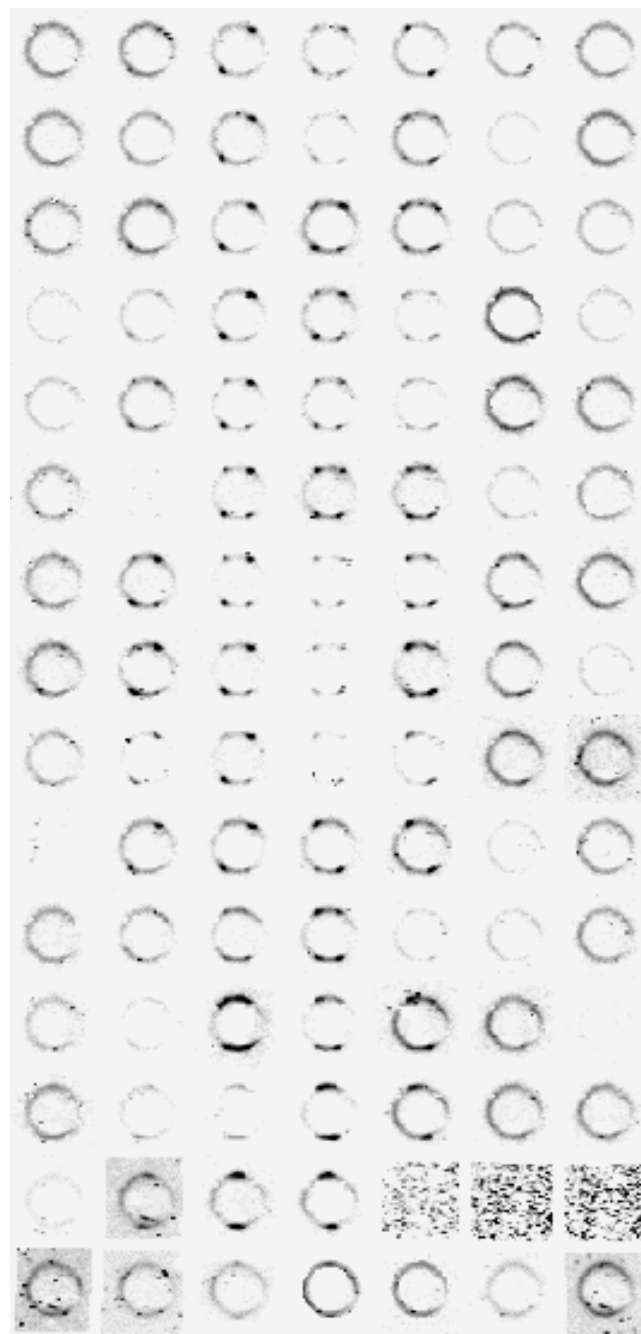


**Figure 10:** SAXS-patterns from scanning the bâtonnet of PEI-1.

From the array of SAXS diagrams in Figure 10, a scheme of the internal bâtonnet structure can be derived which is presented in Figure 11.

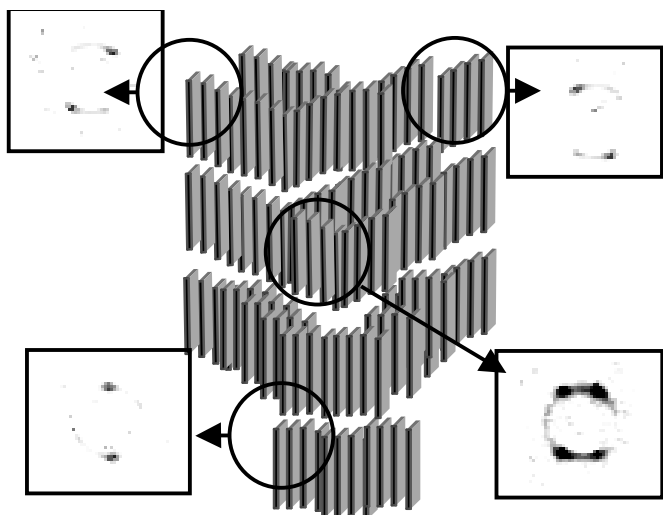


**Figure 11.** Schematic representation of the mesogen arrangement in a PEI-1 bâtonnet and resulting SAXS-patterns at different micro-focus beam positions on the sample (the circle sketches the beam profile)

### 3.3 Smectic Spherulite

In PEI-2, the smectic-crystalline phase develops directly from the isotropic melt without an intermediate LC-phase. Starting from nuclei, spherulites grow with an internal smectic layer order, which is more complex than in PEI-1.

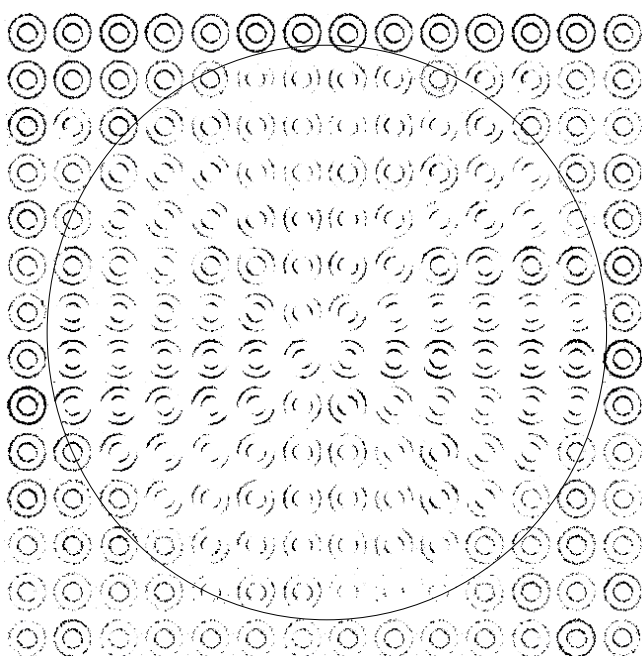


**Figure 12.** Array of SAXS-diagrams of a smectic PEI-2 spherulite, the circle sketches the borderline of the spherulite to the surrounding matrix; step size is 9  $\mu\text{m}$  per frame.

Due to the alternating sequence of two aliphatic and two aromatic segments, a quadruple layer structure is formed, which gives rise to two SAXS reflections at  $2\theta = 2$  and  $4^\circ$ , resp..

A very large PEI-2 spherulite was grown by isothermal crystallization, quenched rapidly, and scanned with the micro-focus X-ray camera. The map of SAXS patterns in Figure 12 visualizes the orientation of the smectic layers within the spherulite. As expected from the nucleation-induced phase growth, the smectic layers exhibit a preferred radial orientation. In the centre of the spherulite, the anisotropy of the scattering is lost due to the fanned structure of the nucleus. The matrix appears isotropic as well, since the size of the crystalline aggregates formed during quenching is smaller than the beam diameter.

### 4. Conclusions

The novel micro-focus x-ray scattering technique is a powerful tool for the investigation of polymer morphology. The azimuthal distribution of the X-ray reflections provide information on the local molecular order and orientation. Scanning LC-textures and mapping the resulting SAXS-patterns visualises the arrangement of the smectic layers. In the glassy state of a PEI-1 Schlieren-texture, the local director field could be examined and parameters of the domain texture, like type and density of defects and were evaluated. Bâtonnets of PEI-1 are characterised as a highly symmetrical shape of layer arrangement, which is demonstrated via maps of SAXS-patterns. They exhibit an internal smectic LC-structure ( $S_C$ ) in which the layer normals are tilted with respect to the bâtonnet axis. Furthermore, smectic-crystalline spherulites of PEI-2 were grown by crystallisation from nuclei out of the isotropic melt. These spherulites have an internal smectic layer structure within the lamellae. The director (SAXS-reflection) changes gradually within the spherulitic regions. Within the spherulite, it indicates a preferred orientation of the layers parallel to the growth direction, whereas the centre (nucleus) appears isotropic.

<sup>1</sup>Gray, G. W., Goodby, W. G., *Smectic Liquid Crystals*, Leonard Hill, New York (1984).

<sup>2</sup>DeGennes, P. G, Prost, J., *The Physics of Liquid Crystals*, 2<sup>nd</sup> ed. Oxford University Press (1993)

<sup>3</sup>C. Wutz, *Polymer* **39** (1) (1998), 1-6.

<sup>4</sup><http://www.esrf.fr/cgi-bin/blhand?BEAMLINE=b11&DOC=handbook>

<sup>5</sup>H.R. Kricheldorf, R. Pakull, G. Schwarz, *Makromol. Chem.*, **194** (1993), 1209.

<sup>6</sup>Riekell, C., *SPIE* **181** (1993), 1740.